NASA Technical Memorandum 101398

Influence of Alloying Elements on the Oxidation Behavior of $NbAl_3$

M.G. Hebsur
Sverdrup Technology, Inc.
NASA Lewis Research Center Group
Cleveland, Ohio

and

J.R. Stephens, J.L. Smialek, C.A. Barrett, and D.S. Fox
National Aeronautics and Space Administration
Lewis Research Center
Cleveland, Ohio

Prepared for the
Workshop on the Oxidation of High-Temperature Intermetallics
sponsored by the Cleveland Chapter of ASM International and NASA Lewis Research Center in cooperation with Case Western Reserve University, The Metallurgical Society of AIME, and the Cleveland Chapter of TMS-AIME
Cleveland, Ohio, September 22-23, 1988

NASA

INFLUENCE OF ALLOYING ELEMENTS ON THE OXIDATION BEHAVIOR OF $NbAl_3$

M.G. Hebsur
Sverdrup Technology Inc.
NASA Lewis Research Center Group
Cleveland, Ohio 44135

and

J.R. Stephens, J.L. Smialek, C.A. Barrett and D.S. Fox
National Aeronautics and Space Administration
Lewis Research Center
Cleveland, Ohio 44135

E-4275

Abstract

$NbAl_3$ is one candidate material for advanced aeropropulsion systems because of its high melting point (~1685 °C), low density (4.5 gm^2/cm^3), and good oxidation resistance. Although $NbAl_3$ has the lowest oxidation rate among the binary Nb-Al alloys, it does not form exclusive layers of protective Al_2O_3 scales. Recently Perkins et al. have shown the feasibility of forming alumina scales on Nb-Al alloys at greatly reduced Al contents. However, the objective of our investigation was to maintain the high Al content, and hence low density, while achieving the capability of growing protective alumina scales. Alloy development followed approaches similar to those used successfully for superalloys and oxidation resistant MCrAlY coatings.

Among the three elements examined (Ti, Si, and Cr) as ternary additions to $NbAl_3$, Cr was the most effective in favoring the selective oxidation of Al. Nb-41Al-8Cr formed exclusive layers of alumina and had a k_p value of 0.22 $mg^2/cm^4 \cdot hr$ at 1200 °C. The addition of 1 wt % Y to this alloy was also beneficial, resulting in nearly an order of magnitude decrease in k_p at 1200 °C. Further improvements were achieved by adding about 1 wt % Si to the quaternary alloy. The k_p value of 0.012 $mg^2/cm^4 \cdot hr$ for Nb-40Al-8Cr-1Y-1Si at 1200 °C was identical to the best NiAl+Zr alloys. These $NbAl_3$ alloys also exhibited excellent cyclic oxidation resistance for 100 hr at 1200 °C, being nearly equivalent to NiAl+Zr.

Introduction

NASA Lewis has recently initiated a High Temperature Engine Materials Program (HITEMP) to develop materials for advanced gas turbine engine applications. At the present time, nickel-base superalloys are the most widely used in aircraft engines where they can withstand temperatures up to 1100 °C. In order to extend the use temperature to 1600 °C, increase efficiency, and reduce fuel costs, advanced ceramics and refractory metals are being considered. Revolutionary materials such as ceramic matrix composites show some potential in terms of thermal capability and strength/weight ratio; however, they also present high risks in terms of reliability. Refractory metals or intermetallic compounds offer another possibility of high temperature matrix materials.

Among the refractory metals, niobium and niobium alloys are the most attractive because of their favorable combination of density, high melting temperature, cost and availability. However, niobium-base alloys oxidize very rapidly above 650 °C. Also, they are embrittled by oxygen, carbon and nitrogen. While niobium alloys can be coated with an oxidation resistant silicide such as $MoSi_2$, coating performance and reliability are not satisfactory for advanced gas turbines where long lives at high temperatures are required.

The oxidation behavior of Nb-alloys was the subject of considerable research in the period 1955 to 1970 (1). The understanding of the oxidation of Nb-Al alloys with particular emphasis on the selective oxidation of Al is a recent one. Svedburg's (2) investigation in 1976 found that the slowest oxidation rate of all Nb-Al compounds was observed for $NbAl_3$ at 1200 °C. Although an inner layer of alumina forms on $NbAl_3$ adjacent to the metal-oxide interface, an $AlNbO_4$ outer layer forms at the oxide-gas interface. Also the parabolic scaling constant, k_p, at 1200 °C for $NbAl_3$ was about 1.01 $mg^2/cm^4 \cdot hr$ which is two orders of magnitude higher than NiAl, an alloy that forms a protective alumina scale at 1200 °C. Recently Perkins et al. (3) have shown the feasibility of forming compact, adherent alumina scales on Nb-Al alloys at greatly reduced Al contents, but only above 1400 °C. The k_p values for these alloys were still quite high, especially at low temperature, even higher than that of $NbAl_3$.

The overall objective of this program is to develop low density Nb-Al alloys with alumina-forming capability and consequently greatly improved oxidation resistance. These alloys may be used either as matrices, if adequate ductility and strength requirements are met in fiber reinforced composites for 1400 °C structural applications, or as a coating on structural alloys of niobium.

In the first phase of this program, the goal is to identify the most oxidation resistant and ductile composition of niobium aluminide produced by conventional casting techniques. Nb-Al alloys processed by conventional casting have a tendency to exhibit segregation of the alloying constituents and coarse grain structures, and hence suffer from severe embrittlement resulting in limited engineering properties. It is also difficult to fabricate test specimens from these brittle materials. Rapid solidification is being considered as a means to obtain homogeneous and fine grained microstructure which not only may decrease the rate of oxidation by increasing the grain boundary diffusion of Al in order to enhance Al_2O_3 scale formation, but also may improve the ductility and strength of the alloy. Therefore, in the second phase of this program, rapid solidification processing of selected compositions from the first phase will be carried out using chill block melt spinning techniques.

In the present investigation, which forms only a part of the first phase, the aim was to study the effect of alloying additions on the oxidation behavior of conventionally cast $NbAl_3$ base alloys. These studies will help to identify the compositional and structural factors that control the selective oxidation of Al to form protective alumina scales.

Experimental Details

Alloy Preparation

All experimental alloys were prepared by induction melting in 25 mm o.d. dense alumina crucibles using a 15 kW furnace. A charge of about 100 gm of high purity alloying elements was used. The surfaces of the charge material, prior to placement in the crucible, were ground with 400 grit silicon carbide (SiC) paper, then washed in methanol using an ultrasonic cleaner. About 2 wt % excess Al was added to each charge to compensate for evaporative losses during melting. The furnace was evacuated to 10^{-3} Pa and back filled with high purity argon for three times prior to melting. The molten alloy was allowed to furnace-cool in the alumina crucible. Castings produced by this technique were shiny with no evidence of any surface oxide, but had a small degree of shrinkage porosity and cracks that developed during cooling. Unless stated otherwise, all alloy compositions are given in weight percent. Conversions to atomic percent are listed in Table I. Most of the alloys had very low amounts (less than 100 ppm) of interstitial elements such as oxygen and nitrogen. Complex alloys containing 4 to 5 elements exhibited some segregation of elements particularly at the bottom and top end of the ingot which were rejected during machining. Chemical analyses were carried out using ICP emission spectrometer.

TABLE I. - CHEMICAL COMPOSITION OF Nb-Al ALLOYS

Alloy designation	Composition	
	atomic percent	weight percent
$NbAl_3$	24Nb-75Al	54Nb-46Al
Nb-Al-Cr	24Nb-70Al-6Cr	50Nb-41Al-8Cr
Nb-Al-Ti	24Nb-70Al-6Ti	51Nb-42Al-7Ti
Nb-Al-Si	24Nb-70Al-6Si	53Nb-43Al-4Si
Nb-Al-Cr-Y	24.5Nb-68Al-7Cr-0.5Y	51Nb-40Al-8Cr-1Y
Nb-Al-Cr-Zr	24.5Nb-68Al-7Cr-0.45Zr	51Nb-40Al-8Cr-1Zr
Nb-Al-Si-Zr	25.5Nb-68Al-6Si-0.5Zr	53Nb-42Al-4Si-1Zr
Nb-Al-Cr-Y-Si	24.5Nb-62Al-7Cr-0.5Y-6Si	47Nb-40Al-8Cr-1Y-4Si
Nb-Al-Cr-Y-Si	24Nb-66.9Al-7Cr-0.5Y-1.6Si	50Nb-40Al-8Cr-1Y-1Si

Oxidation Experiments

Rectangular coupons, 1.2 by 0.75 by 0.25 cm with a 0.20 cm diameter hole for hanging in the isothermal and cyclic oxidation furnaces, were prepared from the as-cast ingots by electric discharge machining. The coupons were polished using 600 and 1200 grit SiC papers, cleaned in detergent and then ultrasonically cleaned in alcohol prior to oxidation testing. Isothermal oxidation tests on all experimental alloys were carried out at 1200 °C for 50 hr in air using a continuously recording Cahn 1000 microbalance. Some selected alloys were tested in the temperature range 1000 to 1400 °C for up to 100 hr. The steady state kinetic data obtained from these isothermal tests were fitted by a linear regression technique to a parabolic model of oxidation. Mathematically, the expression is given by

$$\Delta W/A = k_p^{1/2} t^{1/2} \qquad [1]$$

where ΔW is the weight change at any time, t; A is the area of the specimen; and k_p is the parabolic scaling constant. In most cases, the fit produced R^2 values over 0.90.

Cyclic oxidation tests were carried out on some selected alloys at 1200 °C in air for 100 cycles. Each cycle consisted of a 1 hr hold at 1200 °C followed by 20 min cooldown outside the furnace. Details of the cyclic oxidation test facility at NASA Lewis have been described previously (4). Specific weight changes were determined at regular intervals of 15 cycles.

After both types of oxidation tests, the retained oxides on the specimen surface and any collected spall were analyzed by x-ray diffraction (XRD) to determine the oxide phases present. Detailed investigations of the oxide scale and metal were carried out on selected specimens using optical, electron microscopic and electron microprobe techniques.

Results and Discussions

From the 1200 °C/50 hr isothermal test data on $NbAl_3$, the k_p value was calculated to be 0.9 $mg^2/cm^4 \cdot hr$. This value is in close agreement with that of Svedberg (2) reported earlier. XRD result on oxidized specimen showed the presence of strong peaks of both Al_2O_3 and $AlNbO_4$, a rutile type oxide. Microprobe investigation on the cross section of the oxidized specimen indicated an outer layer of $NbAlO_4$ followed by Al_2O_3 (Figure 1). The alumina scale was not compact and continuous, but layers of Al_2O_3 and $NbAlO_4$ were evident. Similar observations have been documented by Perkins et al. on pure $NbAl_3$ oxidized at 1350 °C for 1 hr (3). They have applied Wagner's model for the transition from internal to external oxidation of Al, to the oxidation of Nb-Al alloys. According to Wagner (5), an external alumina will form when the atom fraction of Al in the Nb-Al binary alloy exceeds the critical value, $N_{Al}^{(o)}$, given by:

$$N_{Al}^{(o)} > \left[\frac{\pi g^*}{3} N_o^{(s)} \frac{D_o V_m}{D_{Al} V_{ox}}\right]^{1/2} \qquad [2]$$

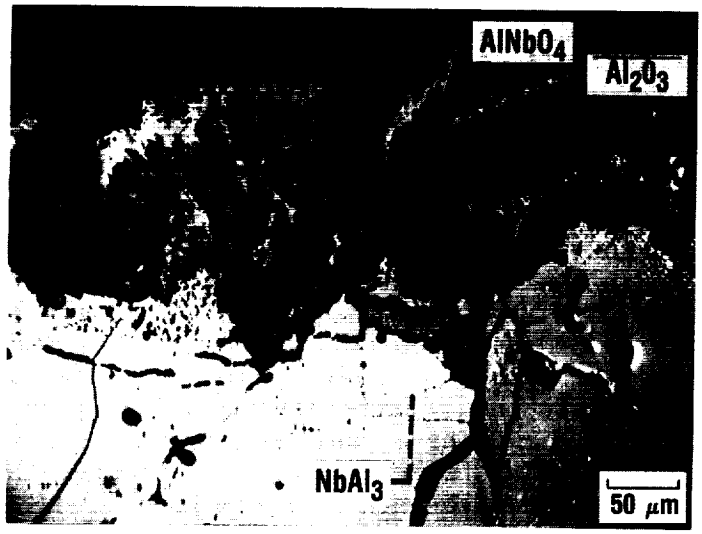

Figure 1 - Oxide scales formed on $NbAl_3$ in air, 1200 °C/50 hrs.

where $N_O^{(s)}$ is the atom fraction of oxygen solubility in the alloy, D_O and D_{Al} are the diffusivities of O and Al in the alloy, respectively, V_m and V_{ox} are the molar volumes of the alloy and oxide, respectively, and g^* is the critical volume fraction of the oxide required to form a healing layer. By decreasing the oxygen solubility and diffusivity, and by increasing the diffusivity of Al in the alloy, external alumina scales will be promoted. Alloying additions can therefore be chosen such that they influence the above three factors in favor of alumina scale formation.

The oxygen solubility, may be decreased through a gettering effect of a third element, such as Ti or Si, the oxides of which are intermediate in stability between Al_2O_3 and Nb_2O_5. Elemental additions that increase the electron concentration in Nb, such as Cr and W also may effectively decrease the oxygen solubility by increasing the activity of oxygen (6). Based on the trapping energy model (7), solutes with more negative enthalpies of formation of their oxides (such as Hf) and smaller atomic radii than Nb (such as Cr) may decrease the oxygen diffusivity, D_O, by providing attractive traps.

There has been no systematic study to assess the influence of alloying elements on the diffusion of Al in Nb. However, an increased Al content and increased temperature may increase the value of D_{Al}. Also, increasing the solubility of Al in bcc Nb by the addition of alloying elements such as Cr, Ti and Fe may favorably increase the diffusivity of Al (6).

Based on these arguments, Cr, Si and Ti appear to be the first choice as additions to improve the oxidation behavior of $NbAl_3$. About 6 at % of each element was added to $NbAl_3$. Figure 2 shows the typical microstructures of the ternary alloys. Ternary additions tend to form a complex intermetallic phase along the grain boundaries. Figure 3 shows the values of parabolic scaling constants, k_p, obtained from isothermal tests at 1200 °C for each alloy. It is clear from Figure 3 that Cr and Si have reduced the k_p values by more than 50 percent. XRD analysis of the oxidized surface indicate strong presence of Al_2O_3 (Table II). Figure 4 shows the microstructure of the oxidized Nb-43Al-4Si specimen. Although this alloy forms continuous Al_2O_3 scales (as confirmed by microprobe analysis), extensive internal oxidation of Al occurred along the Si-rich phase.

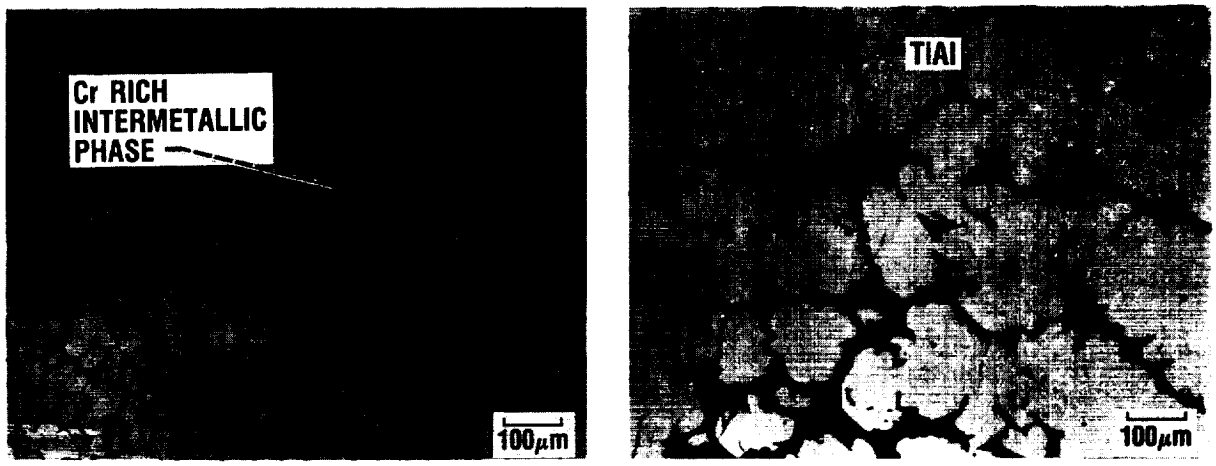

Nb-41-8Cr Nb-42Al-7Ti

Figure 2 - Optical micrographs of as-cast Nb-Al-X alloys.

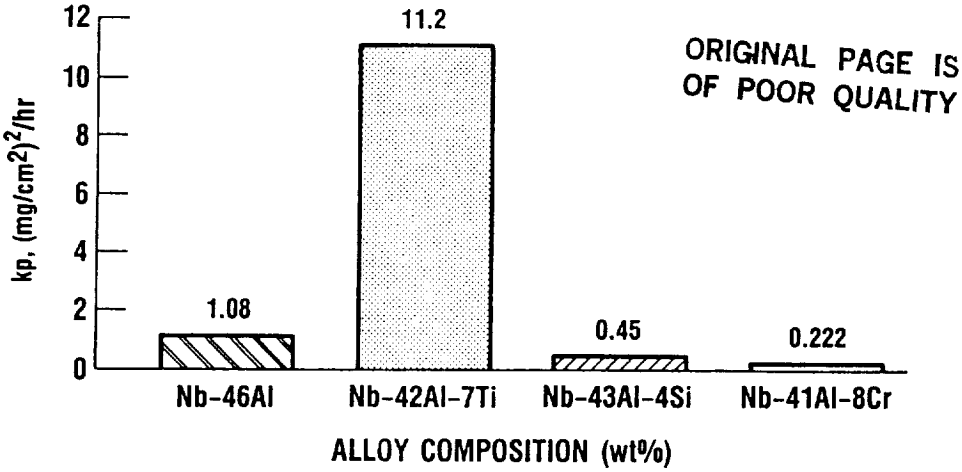

Figure 3 - Effect of ternary addition on the oxidation rates of $NbAl_3$.

TABLE II. - OXIDE PHASES FORMED ON EXPERIMENTAL Nb-Al ALLOYS

Alloy composition, wt %	Oxidation temperature, °C	Oxide phases present
$NbAl_3$(54Nb-46Al)	1200	$AlNbO_4$, Al_2O_3
Nb-42Al-7Ti	↓	$AlNbO_4$, Al_2O_3
Nb-41Al-8Cr		Al_2O_3(s), $AlNbO_4$(m)
Nb-43Al-4Si		Al_2O_3(s), $Nb(AlSi)_2$(m)
Nb-40Al-8Cr-1Y	1000	Al_2O_3(s), $AlNbO_4$(w)
	1200	Al_2O_3(s), $AlNbO_4$(w)
	1400	Al_2O_3, Several unknowns
Nb-40Al-8Cr-1Zr	1200	Al_2O_3(s), $AlNbO_4$(w)
Nb-42Al-4Si-1Zr	↓	Al_2O_3(s), $NbAl_3$(m)
Nb-40Al-8Cr-1Y-4Si		Al_2O_3(s), Unknowns
Nb-40Al-8Cr-1Y-1Si		Al_2O_3(s), Unknowns

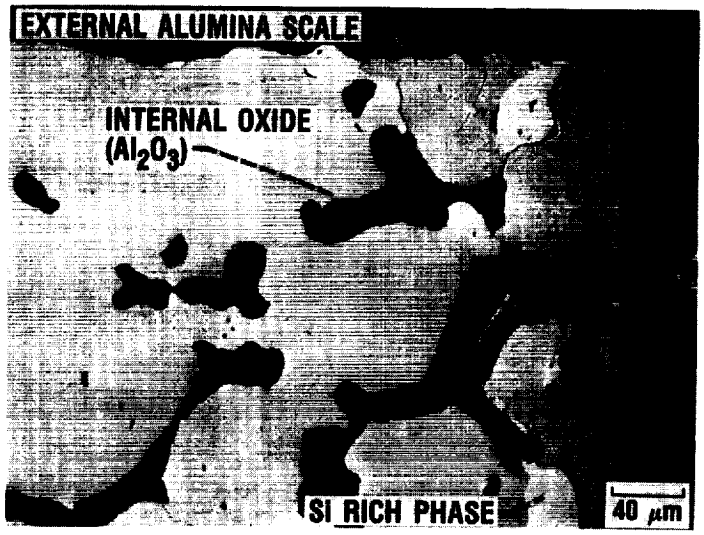

Figure 4 - Electron micrograph (back scatter) of Nb-43Al-4Si showing external and internal oxidation of Al.

The microstructure of oxidized Nb-41Al-8Cr specimen (Figure 5), shows a continuous external alumina scale without any internal oxidation. Microprobe analyses indicates chromium to be present along the grain boundaries as a complex intermetallic phase. Preliminary investigations using selected area diffraction (SAD) indicate that this intermetallic phase has a cubic structure.

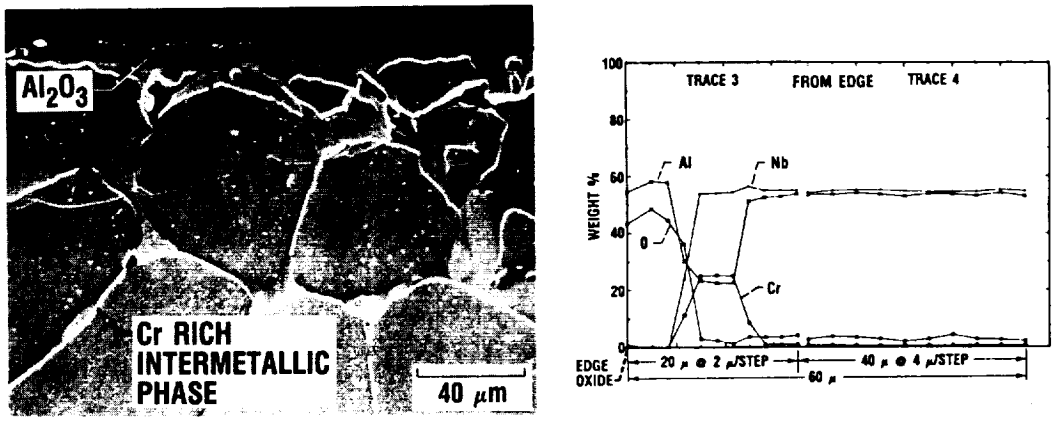

Figure 5 - Electron micrograph (back scatter) of Nb-41Al-8Cr showing a continuous external Al_2O_3 scale and a Cr rich phase along the grain boundaries.

It is known that small additions of oxygen active elements have dramatic effects on the oxidation behavior of NiCrAl alloys (8-9). Thus 1 wt % (0.5 at %) additions of Zr and Y were made to Nb-Al-Cr and Nb-Al-Si alloys. It appears that Y additions refined the grain size of an Nb-40Al-8Cr-1Y alloy, Figure 6. Figure 7 shows a bar chart of k_p values of these quartenary alloys along with the ternary Nb-Al-Si and Nb-Al-Cr alloys. Clearly the oxygen active elements have further reduced the k_p values. This is especially true for the Y-containing alloy, where the k_p values have decreased an order of magnitude.

Figure 8 shows the microstructure of a Nb-Al-Si-Zr alloy oxidized at 1200 °C for 100 hr. Again, as with the ternary alloy, this alloy also produces a continuous external alumina scale as well as islands of internal oxides of Al along the grain boundaries adjacent to silicon rich areas.

The microstructures of a Nb-Al-Cr-Y alloy oxidized at 1200 °C for 100 hr is shown in Figure 9. Clearly a continuous external alumina scale and no internal oxidation are evident. The concentration profiles along the grains indicate distinct Cr and Y rich grain boundary phases.

In Figure 10, an Arrhenius plot of the k_p values of a Nb-Al-Cr-Y alloy obtained as a function of temperature is shown. For the purpose of comparison, similar data for NiAl are also plotted in Figure 10. At higher temperatures, the k_p values for Nb and Ni aluminides are very close; where as at low temperatures, Nb aluminides have much higher k_p values than Ni aluminides. This may be due to the low diffusivity of Al in Nb alloys at lower temperatures (6).

XRD analysis of the Nb-Al-Cr-Y specimen oxidized at 1400 °C for 50 hr revealed predominantly alumina as well as several unknown phases. The microstructure of this specimen shown in Figure 11 indicates an increased depth of oxide penetration, redistribution of grain boundary intermetallic phase and grain growth due to the high temperature exposure.

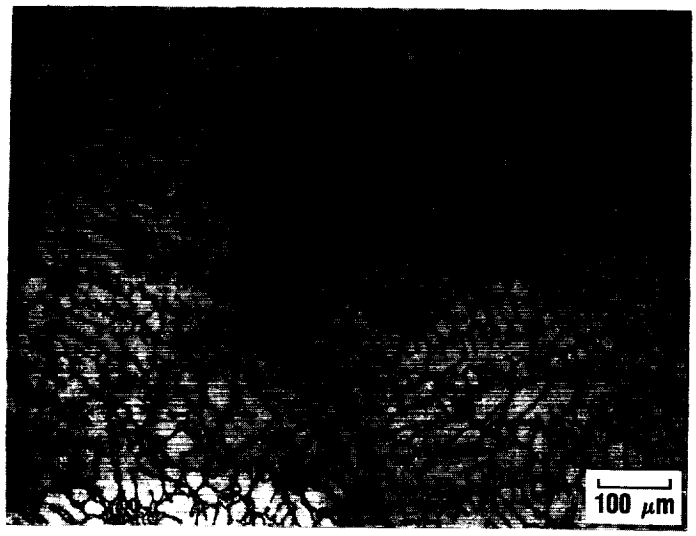

Figure 6 - Optical micrograph of as-cast Nb-40Al-8Cr-1Y alloy.

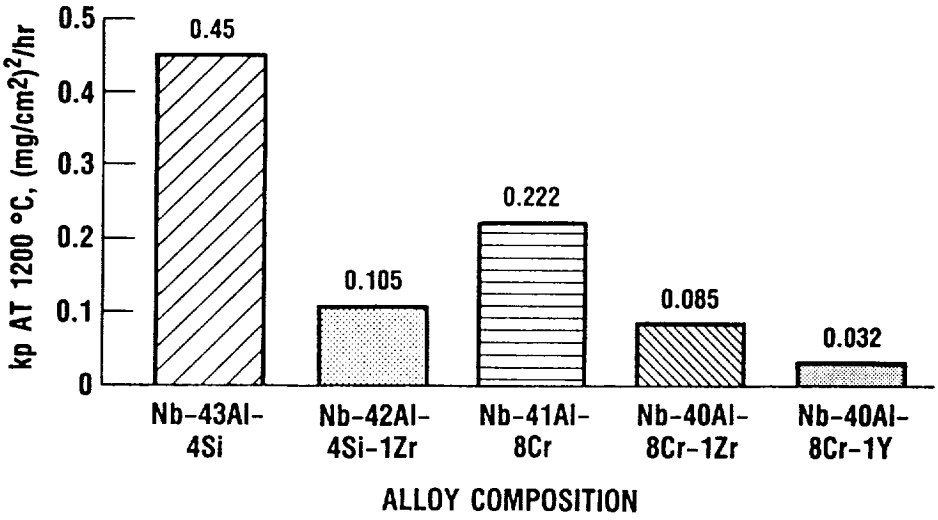

Figure 7 - Effect of Zr and Y additions on the oxidation rates of Nb-Al-Si and Nb-Al-Cr alloys.

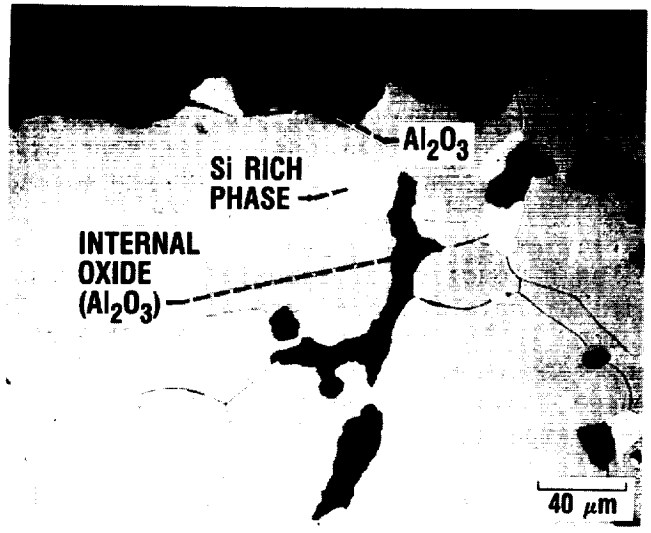

Figure 8 - Electron micrograph (back scatter) of Nb-42Al-4Si-1Zr showing external and internal oxidation of Al.

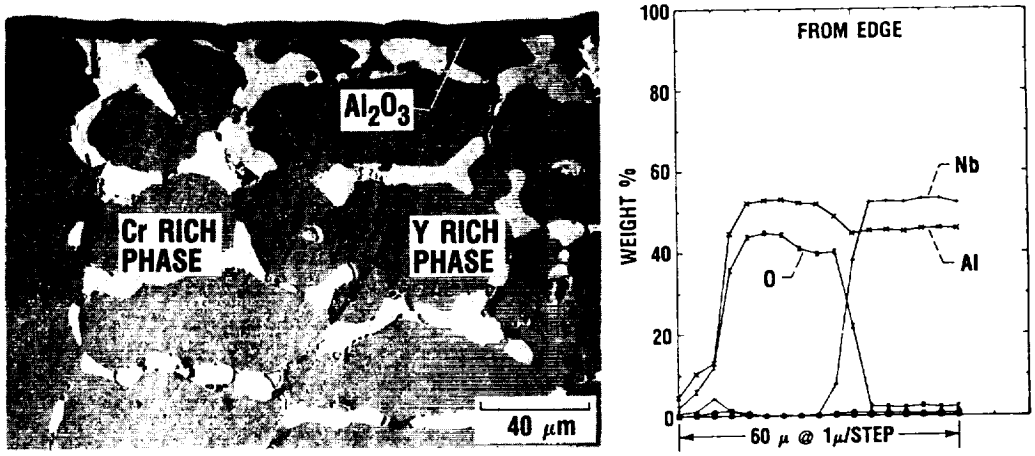

Figure 9 - Electron micrograph (back scatter) of Nb-40Al-8Cr-1Y showing a compact and continuous external Al_2O_3 scale.

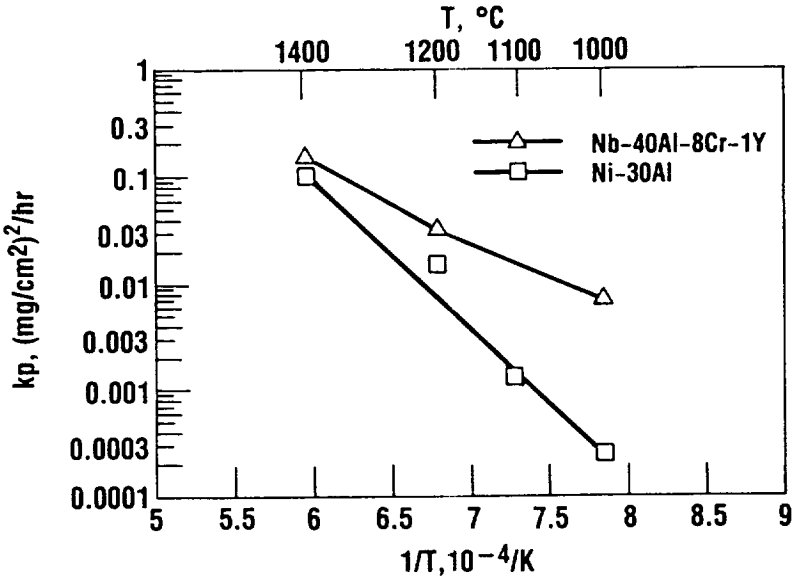

Figure 10 - An Arrhenius plot of k_p for Nb-40Al-8Cr-1Y compared to Ni-30Al.

Figure 11 - Electron micrograph (back scatter) of Nb-40Al-8Cr-1Y oxidized at 1400 °C showing an increased scale thickness and grain growth.

Silicon additions of 1 and 4 wt % (1.6 and 6 at %) were made to the Nb-Al-Cr-Y alloy. Figures 12(a and b) show the optical microstructures of Si containing Nb-Al-Cr-Y alloys. Segregation of excess Si in the form of a complex intermetallic phase can be seen in the alloy containing 4 wt % silicon (Figure 12(a)). The 1200 °C k_p value for the Nb-Al-Cr-Y-4 wt % Si alloy increased by an order of magnitude relative to the k_p value of the Nb-Al-Cr-Y alloy without Si (Figure 13). XRD analysis of the oxidized surface indicated the presence of nonprotective oxides such as $AlNbO_4$ and $CrNbO_4$ along with Al_2O_3. The microstructure of the oxidized specimen is shown in Figure 14, where extensive internal oxidation is evident. On the other hand, an alloy containing only 1 wt % (1.6 at %) Si exhibited a 3-fold improvement in k_p (Figure 13) and no internal oxidation (Figure 15).

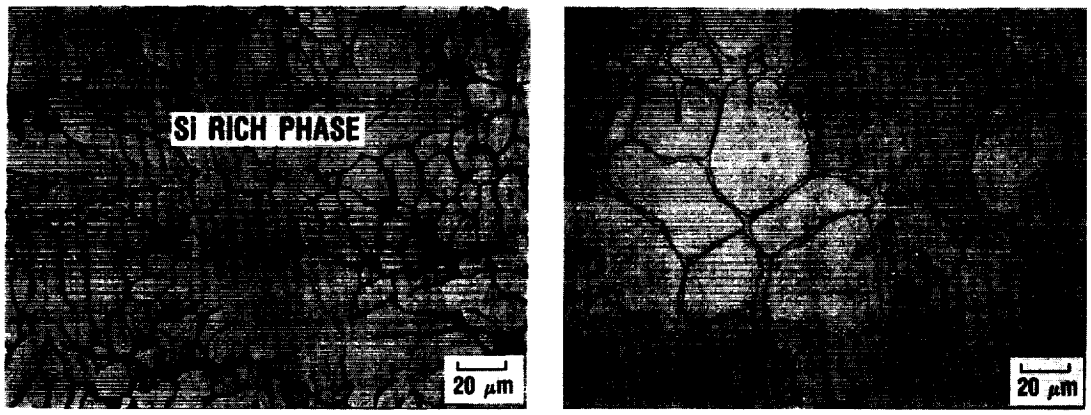

(a) Nb-40Al-8Cr-1Y-4Si (b) Nb-40Al-8Cr-1Y-1Si

Figure 12 - Optical micrographs of as-cast alloys of Nb-40Al-8Cr-1Y containing Si.

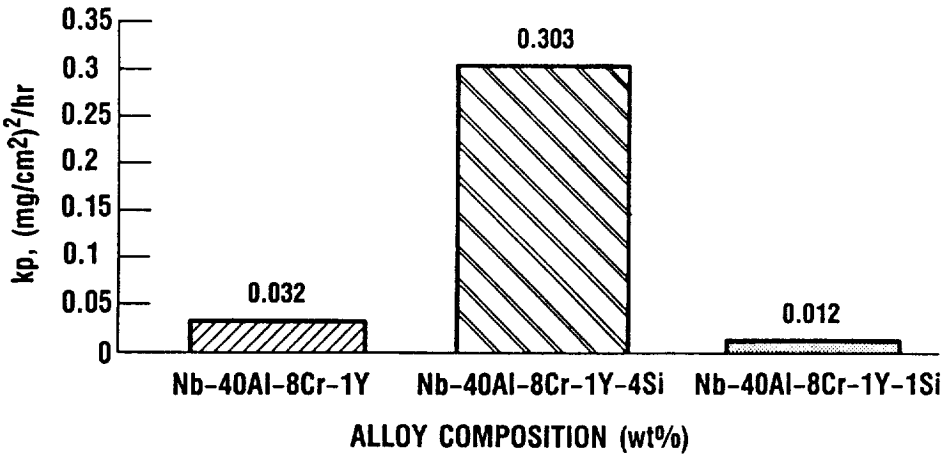

Figure 13 - Effect of silicon additions on the oxidation rates of Nb-40Al-8Cr-1Y alloys.

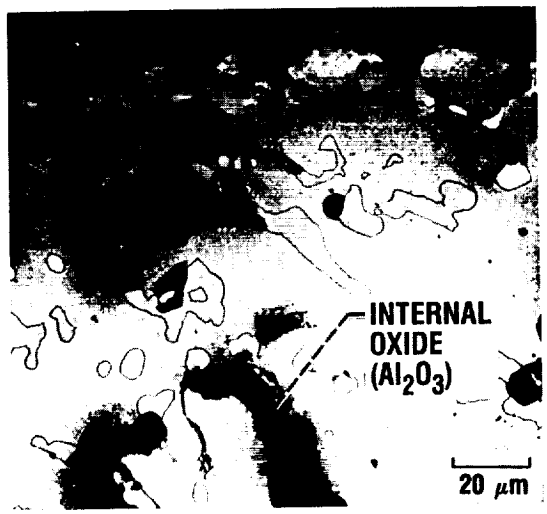

Figure 14 - Optical micrograph of Nb-38Al-8Cr-1Y-4Si showing extensive internal oxidation of Al.

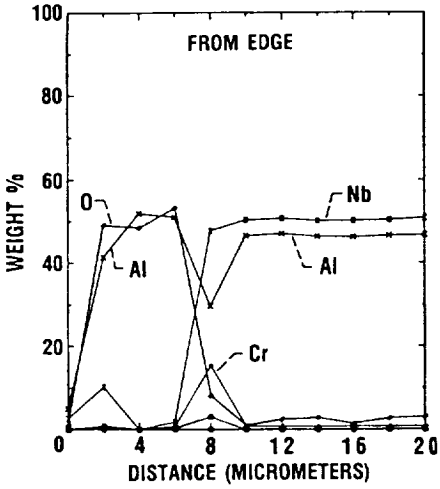

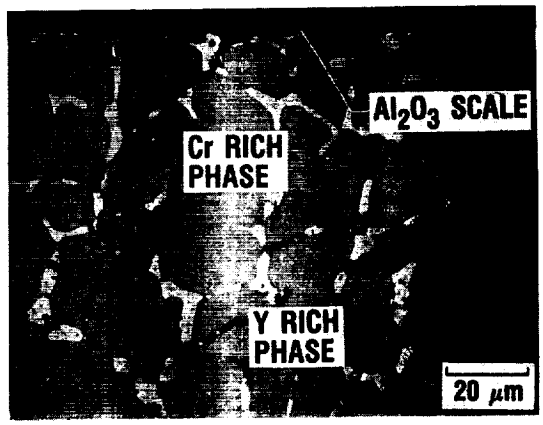

Figure 15 - Electron micrograph (back scatter) of Nb-40Al-8Cr-1Y-1Si showing a continuous external Al_2O_3 scale and no internal oxidation.

Electron microprobe investigations of an alloy containing 4 wt % Si indicated that the matrix of $NbAl_3$ contains up to 1.8 wt % (2.5 at %) Si. The excess Si forms a complex intermetallic phase with Al and Nb. Microprobe analysis of this intermetallic phase estimates about 30Si+12Al+58Nb wt % (45Si+22Al+33Nb at %). Because of the low Al content, this phase and areas adjacent oxidize as a mixture of $AlNbO_4$ and Al_2O_3.

Figure 16 summarizes the isothermal oxidation test results, plotted in terms of relative oxidation rate as a function of alloy composition. For comparison, results of the oxidation of NiAl(10) and Nb-26Al-24Ti-5V-3Cr(6) are also included. It is clear from Figure 16 that the oxidation rate of $NbAl_3$ has been improved by selected alloying additions by nearly two orders of magnitude and is comparable to NiAl. Cyclic oxidation test results of Nb-Al alloys showed the same trend of improvement with the addition of alloying elements as observed in the isothermal tests. Figure 17 shows the plot of the specific weight change versus time for Nb-Al alloys and on Ni-Al alloys as provided by Barrett (10) for comparison. Clearly the Nb-Al-Cr-Y-Si alloy has cyclic oxidation resistance comparable to that of the best alloy, namely NiAl+0.1Zr.

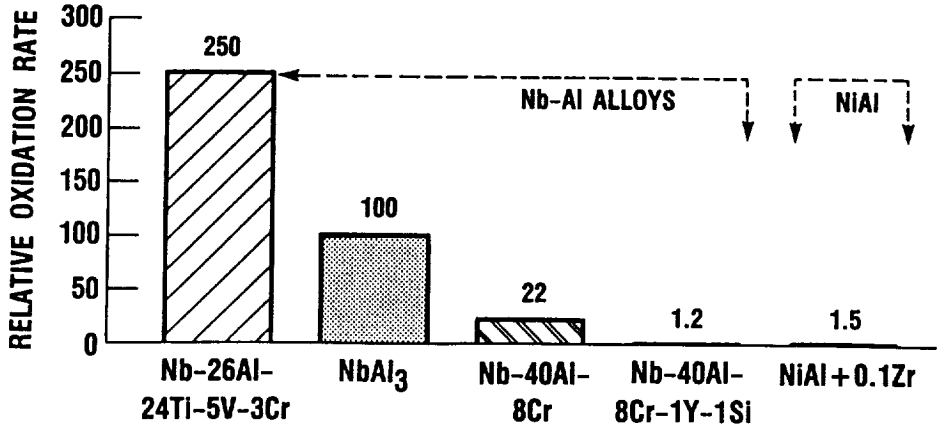

Figure 16 - Comparison of relative oxidation rates of Nb-Al alloys and Ni-Al alloys at 1200 °C.

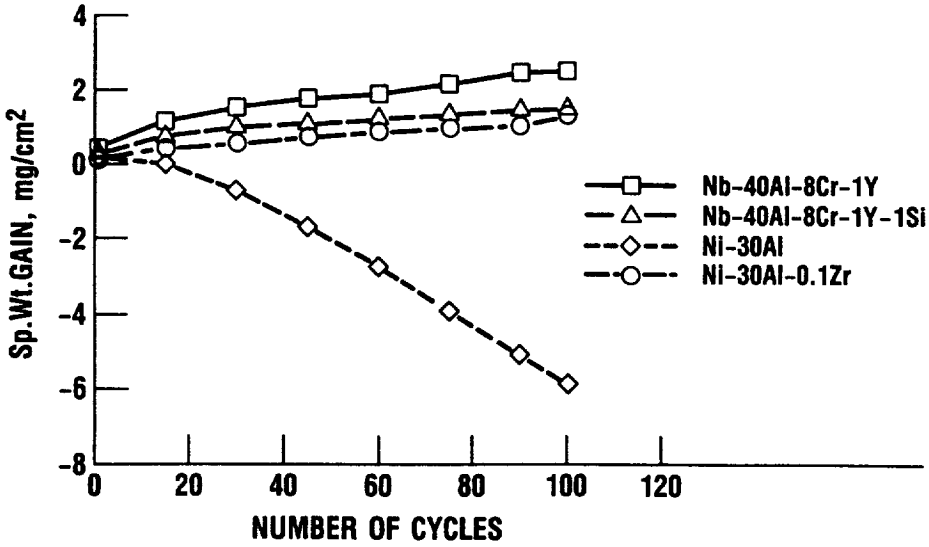

Figure 17 - Cyclic oxidation data of Nb-40Al-8Cr-1Y alloys compared to Ni-30Al and Ni-30Al-0.1Zr alloys.

Concluding Remarks

Pure $NbAl_3$ does not form a protective alumina scale exclusively. By alloying to favor the selective oxidation of Al, a continuous alumina scale can be grown on Nb-Al alloys. As a ternary addition to $NbAl_3$, Cr was more effective than Ti and Si in favoring the selective oxidation of Al. Oxygen active elements had beneficial effect on the oxidation behavior of niobium aluminides. Yttrium was more effective than zirconium. 1200 °C cyclic and isothermal oxidation rates of a Nb-40Al-8Cr-1Y-1Si alloy were comparable to those of a highly oxidation resistant aluminide, NiAl+0.1Zr.

Acknowledgements

The authors would like to thank Henry Geringer, Ralph Garlick, Frank Terepka, and Don Humphrey for their help during various stages of experimentation.

REFERENCES

1. J.F. Stringer, "High Temperature Corrosion of Aerospace Alloys," (AGARD AG-200, Advisory Group for Aerospace Research Development, NATO, Paris, France, 1975).

2. R.C. Svedberg, "Oxides Associated With the Improved Air Oxidation Performance of Some Niobium Intermetallics and Alloys," Properties of High Temperature Alloys, ed. Z.A. Foroulis and F.S. Pettit, (Pennington, NJ: Electrochemical Society, 1976), 331-362.

3. R.A. Perkins, K.T. Chiang, and G.H. Meier, "Formation of Alumina on Nb-Al Alloys," Scripta Metallurgica, 22 (1988) 419-424.

4. C.A. Barrett and C.E. Lowell, "High Temperature Cyclic Oxidation Furnace Testing at NASA Lewis Research Center," Journal of Testing and Evaluation, 10 (1982) 273-278.

5. C. Wagner, "Reaktionstypen bei der Oxydation van Legierungen," Zeitschrift fur Electrochemie, 63 (1959) 772-790.

6. R.A. Perkins, K.T. Chiang, and G.H. Meier, "Effect of Alloying, Rapid Solidification, and Surface Kinetics on the High Temperature Environmental Resistance of Niobium," (LMSC-F195926, Lockheed Missiles and Space Co. Inc., Palo Alto, CA, Feb. 1987). (Also, AFOSR-TR-87-0311).

7. R.J. Lauf and C.J. Altstetter, "Diffusion and Trapping of Oxygen in Refractory Metal Alloys," Acta Metallurgica, 27 (1979) 1157-1163.

8. A.S. Khan, C.E. Lowell, and C.A. Barrett, "The Effect of Zirconium on the Isothermal Oxidation of Nominal Ni-14Cr-24Al Alloys," Journal of the Electrochemical Society, 127 (1980) 670-679.

9. J.L. Smialek and R. Browning, "Current Viewpoints on Oxide Adherence Mechanisms," Symposium on High Temperature Materials Chemistry III, ed. Z.A. Munir and D. Cubicciotti, (Pennington, NJ: Electrochemical Society, 1986), 258-272.

10. C.A. Barrett, "The Effect of 0.1 Atomic Percent Zirconium on the Cyclic Oxidation Behavior of Beta-NiAl for 3000 hours at 1200°C," Oxidation of Metals, (in press), 1988.

NASA
National Aeronautics and Space Administration

Report Documentation Page

1. Report No.	2. Government Accession No.	3. Recipient's Catalog No.
NASA TM-101398		

4. Title and Subtitle

Influence of Alloying Elements on the Oxidation Behavior of $NbAl_3$

5. Report Date

6. Performing Organization Code

7. Author(s)

M.G. Hebsur, J.R. Stephens, J.L. Smialek, C.A. Barrett, and D.S. Fox

8. Performing Organization Report No.

E-4275

10. Work Unit No.

510-01-01

9. Performing Organization Name and Address

National Aeronautics and Space Administration
Lewis Research Center
Cleveland, Ohio 44135-3191

11. Contract or Grant No.

13. Type of Report and Period Covered

Technical Memorandum

12. Sponsoring Agency Name and Address

National Aeronautics and Space Administration
Washington, D.C. 20546-0001

14. Sponsoring Agency Code

15. Supplementary Notes

Prepared for the Workshop on the Oxidation of High-Temperature Intermetallics sponsored by the Cleveland Chapter of ASM International and NASA Lewis Research Center in cooperation with Case Western Reserve University, The Metallurgical Society of AIME, and the Cleveland Chapter of TMS-AIME, Cleveland, Ohio, September 22-23, 1988. M.G. Hebsur, Sverdrup Technology, Inc., NASA Lewis Research Center Group, Cleveland, Ohio 44135; J.R. Stephens, J.L. Smialek, C.A. Barrett, and D.S. Fox, NASA Lewis Research Center.

16. Abstract

$NbAl_3$ is one candidate material for advanced aeropropulsion systems because of its high melting point (~1685 °C), low density (4.5 gm^2/cm^3), and good oxidation resistance. Although $NbAl_3$ has the lowest oxidation rate among the binary Nb-Al alloys, it does not form exclusive layers of protective Al_2O_3 scales. Recently Perkins et al. have shown the feasibility of forming alumina scales on Nb-Al alloys at greatly reduced Al contents. However, the objective of our investigation was to maintain the high Al content, and hence low density, while achieving the capability of growing protective alumina scales. Alloy development followed approaches similar to those used successfully for superalloys and oxidation resistant MCrAlY coatings. Among the three elements examined (Ti, Si, and Cr) as ternary additions to $NbAl_3$, Cr was the most effective in favoring the selective oxidation of Al. Nb-41Al-8Cr formed exclusive layers of alumina and had a k_p value of 0.22 $mg^2/cm^4 \cdot hr$ at 1200 °C. The addition of 1 wt % Y to this alloy was also beneficial, resulting in nearly an order of magnitude decrease in k_p at 1200 °C. Further improvements were achieved by adding about 1 wt % Si to the quaternary alloy. The k_p value of 0.012 $mg^2/cm^4 \cdot hr$ for Nb-40Al-8Cr-1Y-1Si at 1200 °C was identical to the best NiAl+Zr alloys. These $NbAl_3$ alloys also exhibited excellent cyclic oxidation resistance for 100 hr at 1200 °C, being nearly equivalent to NiAl+Zr.

17. Key Words (Suggested by Author(s))	18. Distribution Statement
Niobium aluminides Alumina scale formers Parabolic scaling constant Isothermal and cyclic oxidation	Unclassified – Unlimited Subject Category 26

19. Security Classif. (of this report)	20. Security Classif. (of this page)	21. No of pages	22. Price*
Unclassified	Unclassified	12	A03

NASA FORM 1626 OCT 86

*For sale by the National Technical Information Service, Springfield, Virginia 22161